International Journal of Bifurcation and Chaos, Vol. 17, No. 10 (2007) 3651–3655

SINGLE-ELECTRON CIRCUITS PERFORMING DENDRITIC PATTERN FORMATION WITH NATURE-INSPIRED CELLULAR AUTOMATA

TAKAHIDE OYA
Graduate School of Engineering, Yokohama National University, Tokiwadai 79-5, Hodogayaku, Yokohama 240-8501, Japan
t-oya@ynu.ac.jp

IKUKO N. MOTOIKE
Department of Complex Systems, Future University — Hakodate, 116-2, Kamedanakano-cho, Hakodate, Hokkaido 041-8655, Japan

TETSUYA ASAI
Graduate School of Information Science and Technology, Hokkaido University, Kita 14, Nishi 9, Kita-ku, Sapporo 060-0814, Japan

Received September 19, 2005; Revised April 6, 2006

We propose a novel semiconductor device in which electronic-analogue dendritic trees grow on multilayer single-electron circuits. A simple cellular-automaton circuit was designed for generating dendritic patterns by utilizing the physical properties of single-electron devices, i.e. quantum and thermal effects in tunneling junctions. We demonstrate typical operations of the proposed circuit through extensive numerical simulations.

Keywords: Morphology; pattern formation; semiconductor; nanoelectronics.

1. Introduction

Ordered complex patterns can easily be observed everywhere in the natural world. Among these, bifurcated and branched patterns formed in open systems often serve as a basis for advanced functional structures. Indeed, these structures are essential for performing particular computational tasks in nature, e.g. structures of a neuron's dendritic tree are responsible for various intelligent computing tasks. Recent advances in neuroscience have revealed that fundamental roles of these dendritic trees include not only the transmission of neuronal signals but also functional computation utilizing multiple properties of membranes and spines (early works can be found in [Mel, 1992] and [Blackwell *et al.*, 1998]). In this paper, to incorporate the functions performed by dendritic trees into neuromorphic hardware, our aim is to develop a single-electron circuit that self-organizes spatial dendritic patterns on a multilayer nanodot array. As the first step, we propose a cellular automaton (CA) model based on a behavioral model of bacteria colonies [Motoike, 2004].

It is difficult to implement a huge amount of physical wiring, i.e. axons and dendrites, on a 2-D semiconductor chip because the wiring is fabricated by stacking several layers of only wiring. Here we use single-electron circuits, which are believed to have potential for next-generation VLSIs, to increase the wiring density. We also actively incorporate quantum effects and sensitivity to thermal noise into the design of compact unit circuits for the proposed CA.

2. Model of Cellular Automata for Generating Dendritic Patterns

One of the features of neurons is the complexity of their forms, such as tree-like, branching dendritic form. The details of dendritic pattern formation in neural systems have been mainly studied from the viewpoint of molecular biology, rather than that of general physics. This kind of branching pattern is also observed in many other systems, including trees, crystal growth, protoplasmic streaming tubes of slime molds, bacterial colonies, and so on. Due to generality of these kinds of patterns several models have been proposed to describe complex branching patterns [Witten & Sander, 1981; Carmeliet & Tessier-Lavigne, 2005; Mimura *et al.*, 2000]. One of the best-known simple models is the diffusion limited aggregation (DLA) model [Witten & Sander, 1981]. Another well-known type of model is the reaction–diffusion (RD) model for the pattern formation of bacterial colonies, which exhibit more diverse patterns than the DLA model [Mimura *et al.*, 2000]. Two methods are used to describe RD systems; one is based on partial differential equations (PDE) [Turing, 1952] and the other on discretized CA [Gerhardt *et al.*, 1990]. Space, time and state variables are generally discrete in the CA model, whereas they are continuous in the PDE representation of the RD system. In this paper, we use CA representation of RD dynamics based on bacterial colony pattern formation to represent dendritic patterns because of the variety of patterns available and its expansibility for device applications.

The skeleton of the RD pattern formation model of a bacterial colony consists of movement/schism of bacteria, diffusion of nutrients, and consumption of nutrients by the bacteria. In the model, the dynamics are described as "reaction", the relationship of the bacteria and the nutrient, and "diffusion", which averages the bacteria or nutrient in the neighborhood. In CA models, the targeted space is divided into discrete areas of named cells. The time evolution of the state of each cell is decided by simple inner- and inter-cell rules, and a dynamic pattern or whole structure is generated from these local interaction rules. The algorithm of our CA model is as follows. Three variables are used to describe the state of the system in each cell; active bacteria (activator) a, inactive bacteria (inactivator, a trace of activator) w, and nutrient (substrate) f. The variables a and w take the digit value $\{0,1\}$, and f takes a digit or multivalue. When there are both a sufficient number of activators in the cell's neighborhood and sufficient substrate in the cell, the state of the activators becomes 1 ($a : 0 \rightarrow 1$), and substrate f is depleted in the next step. After ($a \rightarrow 1$), when the substrate in the cell itself is less than the threshold value as a result of depletion, the activator can no longer sustain an active state, the state of the activators becomes 0 ($a \rightarrow 0$), and the state of the inactivator becomes 1 ($w \rightarrow 1$). The substrate diffuses constantly with fluctuation. When there is insufficient substrate, the activators try to take up the limited substrate. As a result, the cluster of activators divides into several clusters, and a branching pattern appears as the cluster of cells, where inactivator $w = 1$.

3. Single-Electron Device for Generating Dendritic Patterns

To imitate the diffusion of the consumed substance with fluctuation in the model, we used a single-electron reaction–diffusion (SE-RD) device [Fig. 1(a)] [Oya *et al.*, 2005], single-electron boxes (SEBs) [Fig. 1(b)], and single-electron memory (SEM) circuits [Fig. 1(c)] [Oya *et al.*, 2003] to implement the CA rules.

A typical single-electron circuit consists of tunneling junctions, resistances and capacitors.

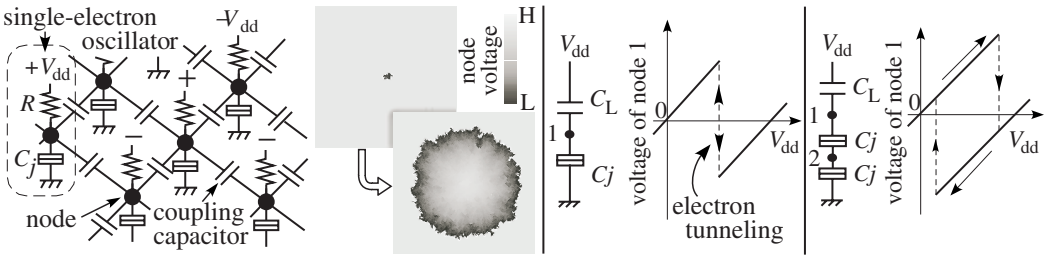

Fig. 1. Single-electron devices. (a) Single-electron reaction–diffusion device, (b) single-electron box, and (c) single-electron memory circuit.

A tunneling junction that is similar to a capacitor is the main component of a single-electron circuit. In a junction, a quantum effect occurs. A point of difference between tunneling junctions and normal capacitors is that the two conductors of the junction face each other very closely. The junction has a threshold voltage value for the generation of a quantum effect that is electron tunneling. A single-electron passes through the junction when the junction potential is over the threshold voltage, and the potential of the junction changes suddenly. The tunneling event has a probability of occurring, given by

$$P(E) \sim \frac{1}{1 - \exp\left[\dfrac{-\Delta E}{k_B T}\right]} \tag{1}$$

where P is the tunneling probability, E is the charging energy, k_B is the Boltzmann constant, and T is the temperature. The equation has a temperature factor. Therefore, the tunneling probability changes with the temperature. In this work, we utilized this physical phenomenon to implement fluctuation in the diffusional operation of the CA model. The left of Fig. 1(a) shows the circuit configuration of a SE-RD device. It consists of arrayed single-electron oscillators with coupling capacitors. The oscillator consists of a tunneling junction, a resistance and a bias voltage source. On the right of Fig. 1(a) is seen a sample operation of the device. The tunneling events propagate randomly when we set input signals that are high enough for single-electrons to tunnel to some nodes. We can generate various patterns on the SE-RD device by setting the device parameters or temperatures to suitable values [Oya *et al.*, 2005]. In this paper, we used this device as a nutrient for the CA model.

We used SEBs to change the input signals to binary signals. The left of Fig. 1(b) shows the circuit configuration of an SEB. It consists of a tunneling junction, bias capacitor, and bias voltage source. The right of Fig. 1(b) shows a sample operation. The SEB shows a positive voltage (logical 1) when no electron tunneling occurs, and a negative one (logical 0) when electron tunneling occurs. We also used SEMs as memory devices because they have a hysteretic function as a function of the input voltage. The left of Fig. 1(c) shows the circuit configuration of an SEM. It consists of two tunneling junctions, a bias capacitor, and a bias voltage source, in series. The right of Fig. 1(c) shows a sample operation [Oya *et al.*, 2003]. The SEBs and SEMs play the role of active and inactive bacteria, respectively.

In this paper, we designed a new single-electron device based on the CA model, the SE-RD device, the SEBs and the SEMs. The device consists of six layers (Fig. 2). We added two factors "$u_{i,j}$" and "$\theta_{i,j}$" to the device as supplementary functions. The first layer consists of arrayed SEBs that implements the "$a_{i,j}$" of the model. The second also consists of arrayed SEBs that implement the added factor "$u_{i,j}$". The third is the SE-RD device, and the fourth consists of arrayed SEMs. The third layer implements "$f_{i,j}$" in collaboration with the fourth layer. In this device, f takes a digit value. The fifth layer consists of arrayed SEBs that implement the added factor "$\theta_{i,j}$", and the sixth consists of arrayed SEMs that implement the "$w_{i,j}$" of the model. The unit circuits of each layer are assumed to be cells of the CA. The operations of each factor are represented by the following equations:

$$a_{i,j} = \begin{cases} 1 & (\text{if } \theta_{i,j} = 1) \\ 0 & (\text{otherwise}) \end{cases} \tag{2}$$

$$u_{i,j} = \begin{cases} 1 & (\text{if } a_{i-1,j} + a_{i+1,j} + a_{i,j-1} + a_{i,j+1} = 1) \\ 0 & (\text{otherwise}) \end{cases} \tag{3}$$

$$f_{RDi,j} = \begin{cases} \text{tunneling} & (\text{if } a_{i,j} = 1 \text{ or neighbor } f_{RD} = \text{“tunneling”}) \\ \text{no tunneling} & (\text{otherwise}) \end{cases} \tag{4}$$

$$f_{i,j} = \begin{cases} 0 & (\text{if } f_{RD\ i,j} = \text{“tunneling” or } f_{i,j} = 0) \\ 1 & (\text{otherwise}) \end{cases} \tag{5}$$

$$\theta_{i,j} = \begin{cases} 1 & (\text{if } \overline{a_{i,j}} \cdot u_{i,j} \cdot f_{i,j} = 1) \\ 0 & (\text{otherwise}) \end{cases} \tag{6}$$

$$w_{i,j} = \begin{cases} 1 & (\text{if } a_{i,j} + w_{i,j} = 1) \\ 0 & (\text{otherwise}) \end{cases} \tag{7}$$

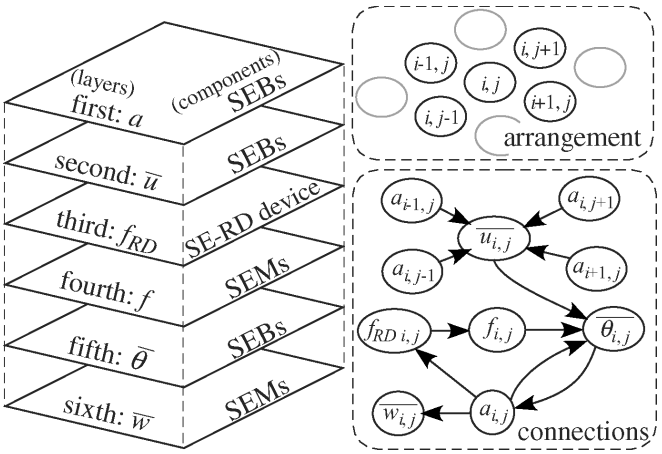

Fig. 2. Single-electron device for generation of dendritic patterns.

4. Results

We tested the operation of the device using computer simulation. In the simulation, the device had 200×200 elements in each layer. Figure 3 shows sample operations of the elements in each layer. In Fig. 3(a), $a_{i,j}$ maintained a logical 0 state (negative voltage) until $\theta_{i,j}$ changed its 0 state to 1 (positive voltage). $u_{i,j}$ kept 0 state until neighbor a changed its 0 state to 1. $f_{i,j}$ ($f_{RDi,j}$) maintained 1 state until $a_{i,j}$ changed its 0 state to 1 or electron tunneling occurred in the neighboring f_{RD} and kept 0 state after it changed its state from 1 to 0. $w_{i,j}$ kept 1 state until $a_{i,j}$ changed its 0 state to 1 and kept 0 state after it changed its state from 1 to 0. Thus, the device implemented the CA model. However,

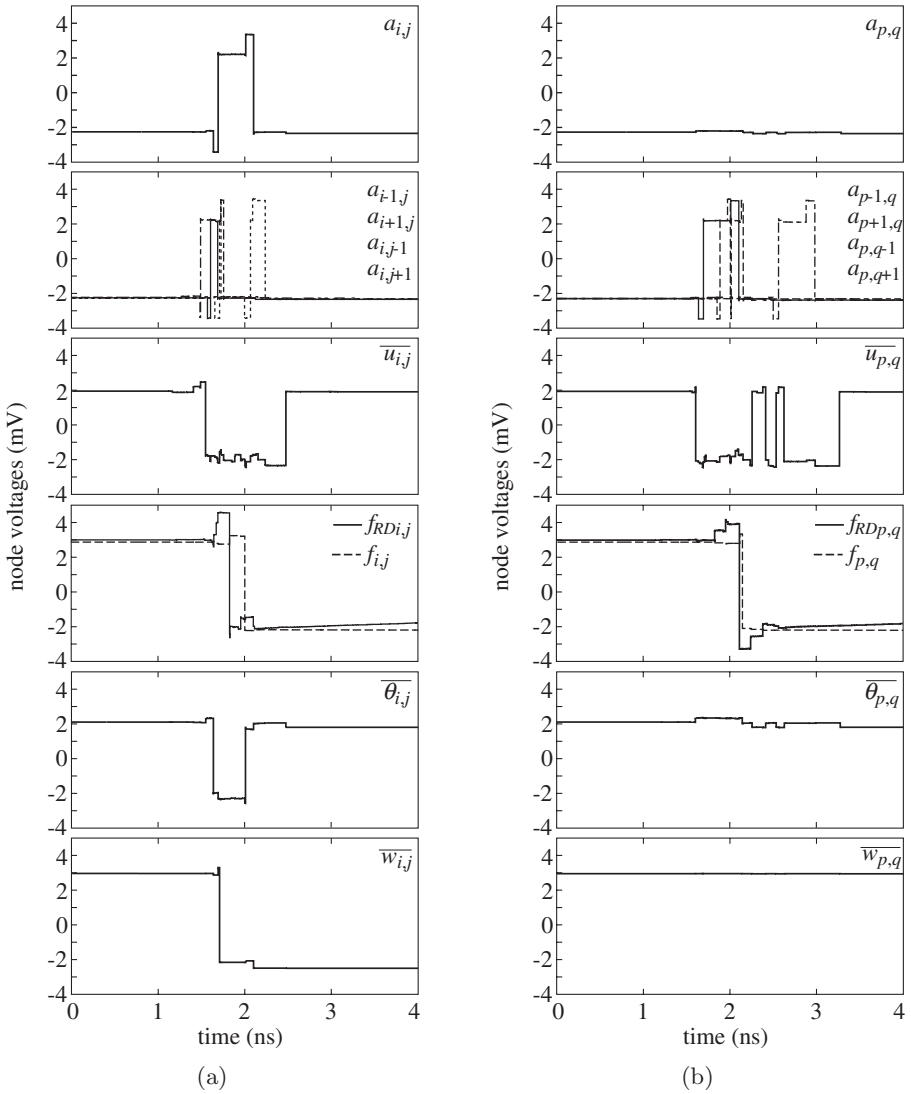

Fig. 3. Simulation results. (a) Correct operations, (b) failed operations.

Fig. 4. Result of two-dimensional simulation of sixth layer.

operating errors sometimes occurred because of the tunneling probability in the device. Figure 3(b) shows sample operations. In the figure, p and q represented different points from i and j. Neighbors a, $u_{p,q}$ and $f_{p,q}$ operated well, as did a, u, f in Fig. 3(a). $\theta_{p,q}$, however, showed a failed operation because of the tunneling probability. As a result, $a_{p,q}$ and $w_{p,q}$ could not change their state. This failed operation works as the diffusion of the consumed nutrient with fluctuation in the model. Figure 4 shows the results of a two-dimensional simulation. In the simulation, a spatiotemporal pattern was formed on the sixth (w) layer. The pattern grew from a planar point, but some parts of the growing points stopped because of both the correct and failed operations in each layer. As a result, a dendritic pattern appeared. This dendritic pattern will change with every simulation because of the tunneling probability.

5. Summary

We proposed novel single-electron circuits for forming dendritic patterns. To construct the proposed device, we designed a six-layer single-electron circuit with nature-inspired cellular automata. The utilized cellular automaton had three factors, a, f and w, which interacted with each other randomly. In the device, the top, second and fifth layers consist of arrayed single-electron boxes, the fourth and sixth layers consist of arrayed single-electron memory circuits, and the third layer is a single-electron reaction–diffusion device. Each layer described each factor (including added factors, u and θ) of the CA rule with randomness. As a result, the device formed dendritic patterns in the sixth layer. These patterns will change with variations in the circuit parameters or temperature environment.

In this paper, we gave no consideration to the number of coupling capacitors between each layer. We now need to consider ways of coupling the unit circuits between the layers. However, coupling capacitors or wires would occupy a huge amount of space in the device. We tested the operation of a device with 200 × 200 elements in each layer, which would need at least 200000 coupling capacitors in total. In future work, we will therefore consider a simpler structure and model for the device.

References

Blackwell K. T., Vogl, T. P. & Alkon, D. L. [1998] "Pattern matching in a model of dendritic spines," *Network*: *Comput. Neural Syst.* **9**, 107–121.

Carmeliet, P. & Tessier-Lavigne, M. [2005] "Common mechanisms of nerve and blood vessel wiring," *Nature* (*London*) **436**, 193–200.

Gerhardt, M., Schuster, H. & Tyson, J. J. [1990] "Cellular automaton model of excitable media II. Curvature, dispersion, rotating waves and meandering waves," *Physica D* **46**, 392–415.

Mel, B. W. [1992] "NMDA-Based pattern discrimination in a modeled cortical neuron," *Neural Comput.* **4**, 502–516.

Mimura, M., Sakaguchi, H. & Matsushita, M. [2000] "Reaction–diffusion modelling of bacterial colony patterns," *Physica A* **282**, 283–303.

Motoike, N. I. [2004] "Generic modeling of dendritic pattern formation with cellular automaton and the property of excitation signal propagation," *Proc. 5th Int. Conf. Biological Physics*, p. 133.

Oya, T., Asai, T., Fukui, T. & Amemiya, Y. [2003] "A majority-logic device using an irreversible single-electron box," *IEEE Trans. Nanotech.* **2**, 15–22.

Oya, T., Asai, T., Fukui, T. & Amemiya, Y. [2005] "Reaction–diffusion systems consisting of single-electron oscillators," *Int. J. Unconvent. Comput.* **1**, 177–194.

Turing, A. M. [1952] "The chemical basis of morphogenesis," *Phil. Trans. R. Soc. Lond. B* **237**, 37–72.

Witten, T. A. & Sander, L. M. [1981] "Diffusion-limited aggregation, a kinetic critical phenomenon," *Phys. Rev. Lett.* **47**, 1400–1403.